Author(s): Guo, Jianpeng & Liu, Huixin & Feng, Xueshang & Pulkkinen, Tuija I. & Tanskanen, E. I. & Liu, Chaoxu & Zhong, Dingkun & Wang, Yuan

Title: MLT and seasonal dependence of auroral electrojets: IMAGE magnetometer network observations

Year: 2014

Version: Final published version

Please cite the original version:

Guo, Jianpeng & Liu, Huixin & Feng, Xueshang & Pulkkinen, T. I. & Tanskanen, E. I. & Liu, Chaoxu & Zhong, Dingkun & Wang, Yuan. 2014. MLT and seasonal dependence of auroral electrojets: IMAGE magnetometer network observations. Journal of Geophysical Research: Space physics, Vol. 119, nro 4. pp. 3179-3188. ISSN 2169-9402 (electronic). ISSN 2169-9380 (printed). DOI: 10.1002/2014JA019843.

AGU PUBLICATIONS

JGR

Journal of Geophysical Research: Space Physics

RESEARCH ARTICLE

10.1002/2014JA019843

Key Points:
- Quiet time currents can contribute to auroral zone geomagnetic perturbations
- EEJ shows a strong MLT variation with significant dependence on season
- WEJ shows a strong MLT variation with significant dependence on season

Correspondence to:
J. Guo and X. Feng,
jpguo@spaceweather.ac.cn;
fengx@spaceweather.ac.cn

Citation:
Guo, J., H. Liu, X. Feng, T. I. Pulkkinen , E. I. Tanskanen, C. Liu, D. Zhong, and Y. Wang (2014), MLT and seasonal dependence of auroral electrojets: IMAGE magnetometer network observations, *J. Geophys. Res. Space Physics*, *119*, 3179–3188, doi:10.1002/2014JA019843.

Received 1 FEB 2014
Accepted 1 APR 2014
Accepted article online 4 APR 2014
Published online 21 APR 2014

MLT and seasonal dependence of auroral electrojets: IMAGE magnetometer network observations

Jianpeng Guo[1,2], Huixin Liu[2], Xueshang Feng[1], T. I. Pulkkinen[3], E. I. Tanskanen[4,5], Chaoxu Liu[1], Dingkun Zhong[1], and Yuan Wang[6,7]

[1]SIGMA Weather Group, State Key Laboratory of Space Weather, CSSAR, Chinese Academy of Sciences, Beijing, China, [2]Department of Earth and Planetary Sciences, Faculty of Sciences, Kyushu University, Fukuoka, Japan, [3]School of Electrical Engineering, Aalto University, Espoo, Finland, [4]Finnish Meteorological Institute, Helsinki, Finland, [5]Department of Physics and Technology, University of Bergen, Bergen, Norway, [6]Key Laboratory of Ionospheric Environment, Institute of Geology and Geophysics, Chinese Academy of Sciences, Beijing, China, [7]Beijing National Observatory of Space Environment, Institute of Geology and Geophysics, Chinese Academy of Sciences, Beijing, China

Abstract Total eastward and westward electrojet currents (EEJ and WEJ) and their central latitudes derived from the International Monitor for Auroral Geomagnetic Effects (IMAGE) network magnetic measurements are analyzed for the combined MLT (magnetic local time) and seasonal dependence during the period 1995–2009. EEJ shows a strong MLT variation with significant dependence on season. During summer months the maxima occur around 1600–1800 MLT, whereas during winter months the maxima occur around 1800–2000 MLT. Moreover, the summer maxima are much larger than the winter maxima and appear at higher latitudes. The summer maxima are mainly associated with the solar EUV conductivity effect, while the winter maxima are mainly due to the contribution of northward convective electric field. EEJ exhibits a dominant annual variation with maximum in summer and minimum in winter. WEJ also exhibits a strong MLT variation with significant dependence on season. The maxima occur around 0200–0400 MLT during summer months, around 0000–0200 MLT during winter months, and around 0000–0400 MLT during equinoctial months. Moreover, the equinoctial maxima are much larger than the summer and winter maxima and appear at relatively lower latitudes. The seasonal variations in WEJ are the combinations of annual variations and semiannual variations. Both annual and semiannual variations show significant dependence on MLT. These results increase our knowledge on what factors contribute to the auroral electrojets as well as their magnetic signatures and hence help us better understand the limitations of global auroral electrojet indices, such as the *AE* and *SME* indices.

1. Introduction

The auroral electrojets are mostly Hall currents flowing approximately in the auroral oval, being eastward in the dusk sector and westward in the midnight and dawn sectors. Occasionally, the westward electrojet is fed by the closure of the substorm current wedge [*Gjerloev et al.*, 2004; *Newell and Gjerloev*, 2011] and shows an extra enhancement in the midnight sector. The magnetic effects of the eastward and westward auroral electrojets can be detected by the magnetometers located on both ground and low-Earth polar-orbiting satellites. This fact leads to the introduction of auroral electrojet indices [e.g., *Davis and Sugiura*, 1966; *Kallio et al.*, 2000; *Tanskanen*, 2009; *Newell and Gjerloev*, 2011] and also forms the basis for the techniques and methods developed to derive the latitude location and intensity of equivalent electrojet currents using the magnetic field measurements [e.g., *Amm and Viljanen*, 1999; *Pulkkinen et al.*, 2003; *Juusola et al.*, 2009; *Vennerstrom and Moretto*, 2013].

The standard auroral electrojet indices (*AU*, *AL*, and *AE*, hereafter called the *AE* indices) were first introduced by *Davis and Sugiura* [1966]. The current *AE* network consists of 12 ground-based magnetometer stations distributed roughly evenly in longitude along the auroral oval region. *AU* and *AL* are defined as the upper and lower envelopes of the superposed H component variations observed at these stations, and *AE* is the difference between the envelopes. Based on their simple definition, *AU* and *AL* are generally assumed to express the strongest current densities of eastward and westward electrojets, respectively. In fact, the strongest auroral electrojets are often undetected when they take place between the *AE* stations, which are not distributed densely in longitude. Thus, in most cases, the *AE* indices are plagued by local time aliasing as

the *AE* stations rotate with the Earth. Furthermore, the *AE* stations cannot properly monitor the auroral electrojets during very active times when they expand equatorward beyond the stations and during quiet times when they contract poleward of the stations [see *Allen and Kroehl*, 1975; *Kamide and Akasofu*, 1983; *Kauristie et al.*, 1996; *Tomita et al.*, 2011; *Liou et al.*, 2013]. In order to improve the *AE* indices, *Newell and Gjerloev* [2011] made great efforts in deriving the auroral electrojet indices using the global network of more than 100 ground magnetometer stations participating in the SuperMAG project [*Gjerloev*, 2009]. The SuperMAG auroral electrojet indices are termed as *SME* indices (*SMU*, *SML*, and *SME*), avoiding confusion with the standard *AE* indices. Despite the large number of stations used in constructing the *SME* indices, significant gaps still exist, which make the *SME* indices also not free from local time biasing.

The auroral electrojets are controlled mainly by the north-south (N-S) component of convective electric field and the Hall conductance over the region. *Ahn et al.* [1999] examined the magnetic local time (MLT) variation of the N-S convective electric field, and found that the northward and southward convective electric fields maximize at about 1900–2000 MLT and 0400–0500 MLT, respectively, and they are nearly symmetric about the 1100 and 2300 MLT meridians. The Hall conductance has two principal sources, namely, solar EUV radiation and auroral particle precipitation. In general, the conductance associated with the solar EUV radiation maximizes near local noon, and that associated with auroral particle precipitation maximizes around local midnight [*Ahn et al.*, 1999; *Guo et al.*, 2012]. Clearly, both the N-S convective electric field and the Hall conductance vary systematically with MLT. Thus, significant MLT variations in the auroral electrojets would be expected. As mentioned above, the MLT effect is one of the major reasons why the *AE* and *SME* indices are limited in use. Therefore, it is important to understand how the auroral electrojets vary with the MLT sector. However, this issue has received little attention in the past decades because of limited magnetic field observations over the auroral oval region.

There are generally two ways to monitor the auroral electrojet currents in all local time sectors, but not simultaneously. The first is utilizing the magnetic field measurements from a single meridional magnetometer chain, such as the International Monitor for Auroral Geomagnetic Effects (IMAGE) magnetometer network [*Viljanen and Häkkinen*, 1997]. When the IMAGE network rotates into a local time sector (~2 h), it can monitor the auroral electrojet activity in its corresponding sector [*Kauristie et al.*, 1996; *Pulkkinen et al.*, 2011; *Guo et al.*, 2012]. After it finishes scanning all local time sectors, it can provide information of the MLT variations of the auroral electrojets. The second way is using the magnetic field measurements from the low-Earth polar-orbiting satellites, such as Oersted, Challenging Minisatellite Payload (CHAMP), and SAC-C [see *Moretto et al.*, 2002]. Recently, *Juusola et al.* [2009] and *Vennerstrom and Moretto* [2013] presented methods to estimate the electrojet currents from the CHAMP magnetic field data. The CHAMP orbit plane drifts roughly 3 h in local time every month. So about 131 days are needed to provide information of the auroral electrojets in all local time sectors. This is a much longer time period when compared to 1 day for the IMAGE network. Therefore, to compare the behavior of the auroral electrojets in different local time sectors under similar solar and geomagnetic conditions, the better choice is magnetic field measurements from the IMAGE network, which is limited to the Northern Hemisphere.

The primary objective of the present study is to investigate the MLT variations in the auroral electrojets using 15 years (1995–2009) of magnetic field measurements from the IMAGE network. This time span covers nearly the whole of solar cycle 23. Considering that the auroral electrojets show significant seasonal variations [e.g., *Ahn et al.*, 2000; *Zhao and Zong*, 2012; *Singh et al.*, 2013; *Guo et al.*, 2014], we will examine the combined MLT and seasonal dependence in the Northern Hemisphere.

2. IMAGE Network Magnetic Measurements

The IMAGE network consists of 31 magnetometers ranging in latitude from 58° (Tartu, Estonia) to 79° (Ny-Ålesund, Svalbard) or from 54° to 75° in corrected geomagnetic coordinates [*Tanskanen*, 2009]. The stations have longitudinal coverage over about 30° from western Norway to the Kola peninsula. Figure 1 shows the locations of the IMAGE magnetometer stations. The coordinates shown are geographic, which will be used throughout the analysis in this paper. The MLT sectors corresponding to the IMAGE network are approximately 2 h later from UT.

The IMAGE magnetometer stations record variations in the geomagnetic field at 10 s cadence. The data are processed to derive equivalent currents by using the spherical elementary current system method [*Amm and Viljanen*, 1999; *Pulkkinen et al.*, 2003]. Then, the total currents of the eastward and westward electrojets

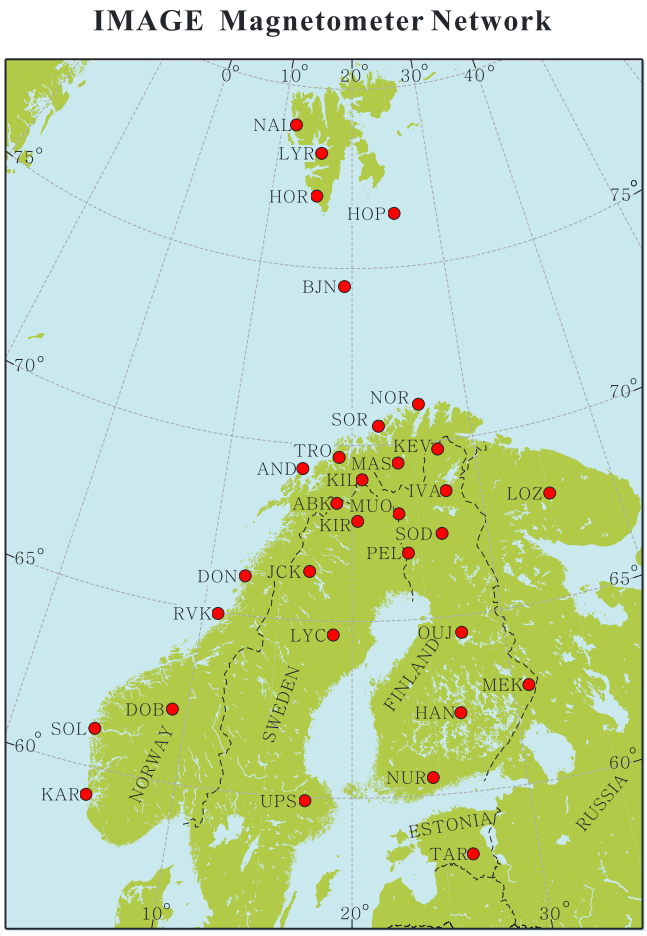

Figure 1. Locations of the IMAGE magnetometer stations (red dots) in geographic coordinates.

(EEJ and WEJ) and their central latitudes (Lat-EEJ and Lat-WEJ) are calculated to study the combined MLT and seasonal dependence. As the IMAGE network can effectively monitor the auroral electrojet activity in MLT sectors ~1200–2200 for the eastward electrojet and ~2200– 0600 for the westward electrojet [*Guo et al.*, 2012], we concentrate on the eastward electrojet in the noon and dusk sectors (1200–2200 MLT) and the westward electrojet in the midnight and dawn sectors (2200–0600 MLT) in the present study. Note that when the IMAGE network is outside these optimal MLT sectors, the strongest magnetic effects of the auroral electrojets are undetected, and thus, the derived electrojet parameters have limited accuracy [see *Kauristie et al.*, 1996; *Guo et al.*, 2012].

In addition, the geomagnetic field data are processed in a way analogous to the *AU*/*AL* indices to produce the *IU*/*IL* indices [*Kallio et al.*, 2000]. Generally, the *IU*/*IL* indices can be used to measure the auroral electrojet intensity but only during limited UT period when the IMAGE network scans their corresponding optimal MLT sectors (mentioned above). However, they are not used as auroral electrojet indices in the present study. They are essentially the peak values of the positive and negative H component disturbances. They and their corresponding latitudes (Lat-*IU* and Lat-*IL*, the latitudes of their contributing stations) are used to characterize the auroral zone geomagnetic disturbances. In this scenario, they are valid in all local time sectors.

3. MLT and Seasonal Dependence of Auroral Electrojets

To investigate the combined MLT and seasonal variations in the auroral electrojets, we calculate the averages of the total currents (EEJ and WEJ) and their central latitudes (Lat-EEJ and Lat-WEJ) over 1 min intervals of MLT in each month. Owing to the quiet time current effects (discussed later), our calculation is limited to the periods when the amplitudes of H component disturbances are larger than 50 nT. The results are shown in Figures 2a–2d for EEJ, Lat-EEJ, WEJ, and Lat-WEJ, respectively, where the standard deviations for the total currents are less than 0.05 megaampere (MA). As we can see, EEJ shows a strong MLT variation with significant dependence on season. During summer months, the maxima with magnitudes about 0.23 MA occur around 1600–1800 MLT. This is expected from the solar EUV conductivity effect [*Ahn et al.*, 2000]. However, during winter months, the maxima with magnitudes about 0.12 MA shift to a later local time sector around 1800–2000 MLT, and they are much smaller than those of summer months. As mentioned earlier, the northward convective electric field maximizes around 1900–2000 MLT, which is consistent with the winter maxima around 1800–2000 MLT. Therefore, it is reasonable to suggest that the northward convective electric field dominates over the Hall conductance in contributing to the winter maxima. Moreover, it is interesting to note that the summer maxima appear at higher latitudes (around 75°N) than the winter maxima do (around 68°N–70°N). Also, as expected, EEJ exhibits a dominant annual variation with maximum in summer and minimum in winter, and the amplitude of the annual variation significantly varies with MLT.

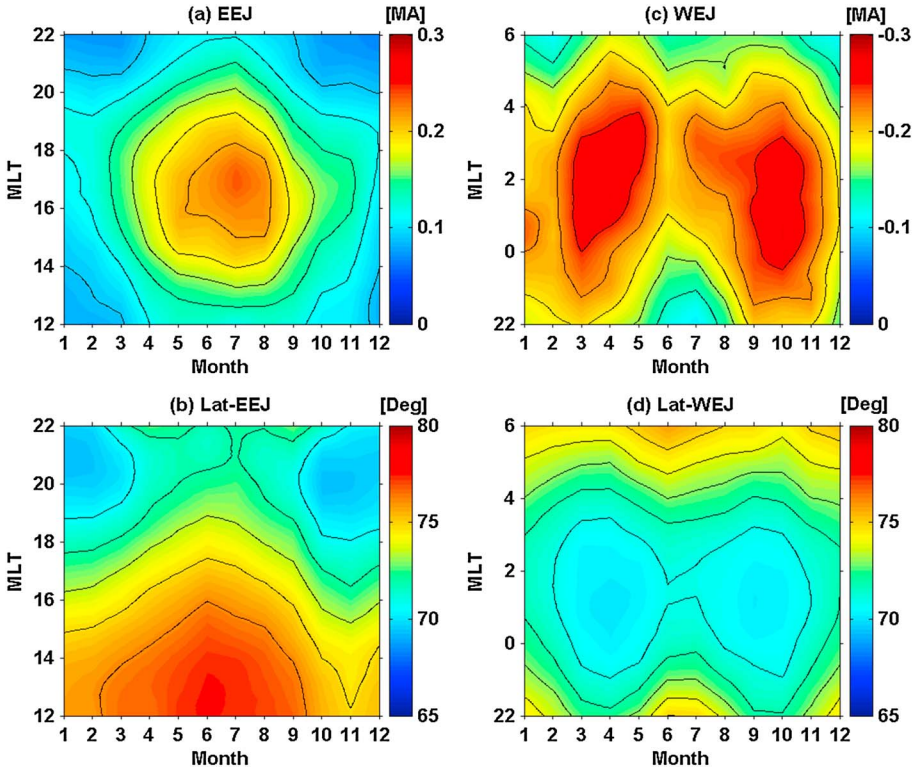

Figure 2. MLT and seasonal variations of the total (a) eastward and (c) westward electrojet currents (EEJ and WEJ) and (b and d) their central latitudes (Lat-EEJ and Lat-WEJ) for the period 1995–2009. Note that the eastward and westward electrojet currents are positive and negative, respectively, and the westward electrojet is plotted in reversed scale such that the magnitude of the current increases upward.

WEJ also exhibits a strong MLT variation with significant dependence on season. The maxima occur around 0200–0400 MLT during summer months, around 0000–0200 MLT during winter months, and in a wider local time sector around 0000–0400 MLT during equinoctial months. Moreover, the equinoctial maxima with magnitudes about 0.28 MA are much larger than the summer and winter maxima with magnitudes about 0.22 MA, and appear at relatively lower latitudes (around 70°N). Certainly, the shift of the central latitude is within 5°. The seasonal variations in WEJ are distinctly visible. More recently, *Guo et al.* [2014] examined the seasonal variations in WEJ and found that they are actually the combinations of annual variations and semiannual variations.

In order to elucidate the annual and semiannual variations, two different band-pass filters, one centered at 365 days with half-power points at 365 $\pm$ 20 days and the other centered at 182 days with half-power points at 182 $\pm$ 20 days, are separately applied to each MLT bin of WEJ. Then the band-pass filtered values are used to calculate the averages over 1 min intervals of MLT in each month. The results are illustrated in Figures 3a and 3b for the annual and semiannual variations, respectively. Obviously, both annual and semi-annual variations show significant dependence on MLT. The annual variations in the MLT sectors 2200–0100 and 0300–0600 are exceptionally strong, while those in the MLT sector 0100–0300 are quite weak. Moreover, it is interesting to note that in the MLT sector 2200–0100 the maximum occurs in winter months and minimum occurs in the summer months, and the opposite is true in the MLT sector 0300–0600. As suggested by *Guo et al.* [2014], the annual variations in the MLT sector 2200–0100 with maxima in winter are caused by the combined effects of the convective electric field and the conductivity associated with particle precipitation, and those in the MLT sector 0300–0600 with maxima in summer are caused by solar EUV conductivity effect and the equinoctial hypothesis (The equinoctial hypothesis is governed by the Ψ angle between Earth-Sun line and the dipole axis of the Earth. When the angle Ψ is further from 90°, the solar wind-magnetosphere coupling is less efficient and the geomagnetic activity is lower [*Svalgaard*, 1977; *Cliver et al.*, 2000; *Finch et al.*, 2008].). The weak annual variations in the MLT sector 0100–0300 could be attributed to the combined effects of annual variations caused by all the previously mentioned effects.

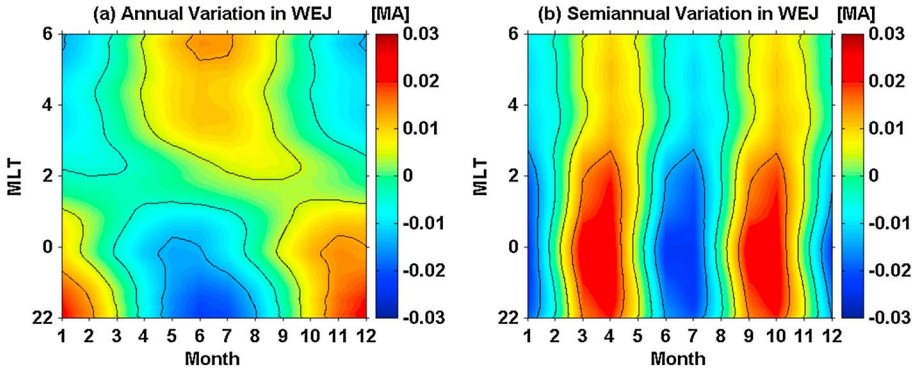

Figure 3. MLT dependence of (a) the annual variation and (b) the semiannual variation in the total westward electrojet current (WEJ).

The semiannual variation in the westward electrojet has been widely studied using the *AL* index [e.g., *Ahn et al.*, 2000]. The most prevailing explanation is the Russell and McPherron (R-M) effect [*Russell and McPherron*, 1973]. The R-M effect is governed by the acute angle between the *z* axis of the GSM coordinate system and the solar equatorial plane, measured in the *y-z* (GSM) plane. A related implication of the R-M effect is that the IMF components in the solar equatorial plane have a peak southward component at the Earth in GSM around March and September, depending on their polarity. However, in many cases the R-M effect has not been able to explain the full seasonal and diurnal variations, which has led to suggestions of the equinoctial hypothesis (mentioned above). One explanation proposed for this is the effect of solar EUV conductivity changes on the nightside auroral electroject [*Lyatsky et al.*, 2001; *Newell et al.*, 2002], acting in addition to the R-M effect.

It should be noted that here no attempt is made to remove the effects of the substorm electrojet. Since the substorm occurrence rate is relatively low and its duration is very short (3 h on average)[*Tanskanen et al.*, 2011], the contribution of the substorm electrojet should have been largely suppressed by our statistical analysis. In order to confirm this, we reexamine the combined MLT and seasonal variations of EEJ and WEJ for the periods when the amplitudes of H component disturbances are between 50 nT and 200 nT. As expected, the results are quite similar to those shown in Figure 2, except for relatively lower amplitudes. This implies that the impact of the substorm electrojet is relatively minor. Since the substorms occur mainly in the premidnight region, roughly 2000–0000 MLT, with maxima during the winter and equinox months and minima during the summer months [*Guo et al.*, 2014], the relatively minor contribution of the substorm electrojet might mainly occur in the premidnight region and during the winter and equinox months. Thus, the MLT and seasonal variations presented in Figures 2 and 3 are mainly associated with convection electrojets. We cannot further examine whether the WEJ reveals similar MLT and seasonal dependence during substorms, because the IMAGE observations cannot monitor the electrojet currents in all local time sectors simultaneously. During substorms, the geomagnetic perturbations recorded by the IMAGE magnetometers in different MLT sectors actually happened in different phases of substorms. Moreover, the electrojet currents derived from the ground-based magnetic measurements have limited accuracy under substorm conditions.

4. Discussion

It is important to remember that the electrojet currents analyzed above are derived from the ground-based magnetic measurements, with an assumption that the auroral zone geomagnetic perturbations are caused only by the auroral electrojets. However, in fact, the quiet time current systems, such as the low-latitude and midlatitude S_q current system and the polar region S_q^p current system, can also contribute to the auroral zone geomagnetic perturbations [see *Allen and Kroehl*, 1975; *Tomita et al.*, 2011]. Therefore, it is necessary to examine whether the quiet time current systems significantly influence the MLT and seasonal patterns of the electrojet currents presented in Figure 2. Considering that the relative contribution of the auroral electrojets and the quiet time current systems might be quite different during quiet and disturbed periods, we separately examine the geomagnetic perturbations for each period. Moreover, we examine the geomagnetic perturbations in all local time sectors, which may help us identify their sources.

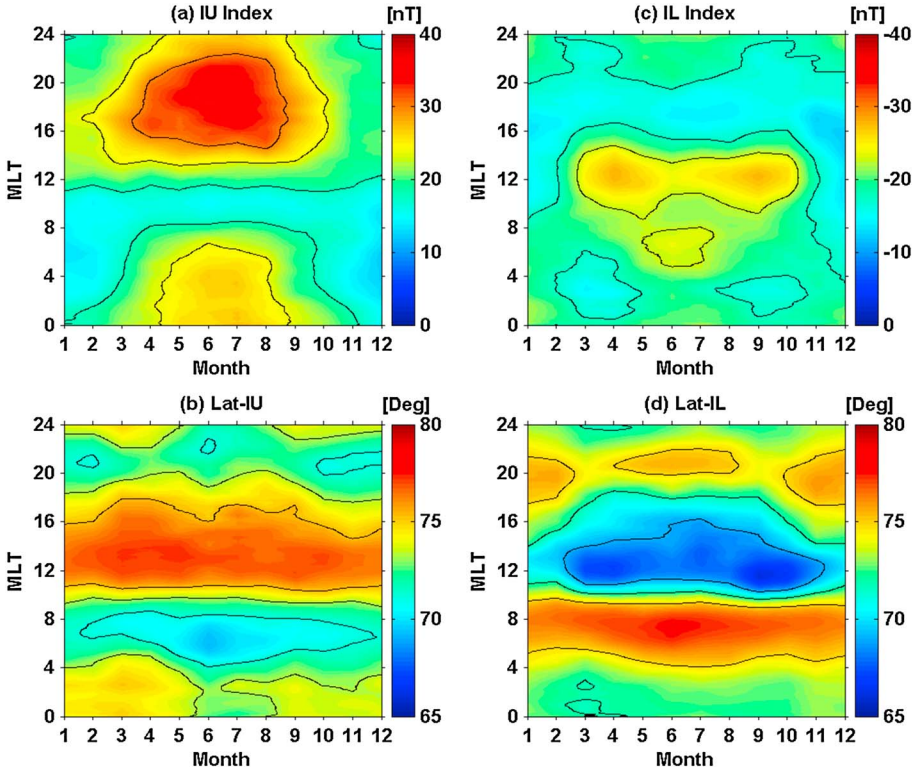

Figure 4. MLT and seasonal variations of the (a) *IU* and (c) *IL* indices and (b and d) their corresponding latitudes (Lat-*IU* and Lat-*IL*) for quiet periods having index values of less than 50 nT. Note that *IU* and *IL* are essentially the peak values of the positive and negative H component disturbances. Here they are used to represent the auroral zone geomagnetic disturbances. *IL* is plotted in reversed scale such that the magnitude of *IL* increases upward.

First, we examine the MLT and seasonal variations of the *IU* and *IL* indices (the peak values of the positive and negative H component disturbances) and their corresponding latitudes (Lat-*IU* and Lat-*IL*) for quiet periods having index values of less than 50 nT. The 50 nT critical level is chosen arbitrarily, but it separates those periods of moderate magnetospheric activity from the quieter periods [see *Allen and Kroehl*, 1975]. The relative weight of quiet periods is about 0.65 (65% of the total) for the *IU* index and 0.62 (62% of the total) for the *IL* index. The results are shown in Figure 4, where the standard deviations for the H component disturbances are no more than 5 nT. Significant seasonal variations can clearly be observed in some local time sectors. For example, the *IU* index reveals annual variations with maxima in summer in MLT sectors 0400–0800 and 1400–0400 (due to different sources discussed below). The *IL* index exhibits annual variations with maxima in summer in the MLT sector 0400–0800, and semiannual variations with maxima at equinoxes as well as annual variations with maxima in summer in the MLT sector 1000–1400. Lat-IL exhibits similar seasonal variations as those observed in the *IL* index in the MLT sector 1000–1400 but with opposite phases. The opposite phase means that Lat-IL shifts equatorward (poleward) as the *IL* index increases (decreases). It is interesting to note that annual variations are observed in both *IU* and *IL* indices in the same MLT sector 0400–0800 but at different latitudes. This indicates that they are caused by different current systems. Also, we note that the values of the *IL* index are very small (less than 15 nT) at equinoxes in the MLT sector 0000–0400 MLT, which suggests that the contributions of the electrojet currents (both eastward and westward electrojets) to the auroral zone geomagnetic perturbations are very minor during quiet periods.

The S_q currents arise due to the ionospheric wind dynamo, and flow at approximately 100–170 km altitude in the sunlit ionosphere [*Pedatella et al.*, 2011]. The morphology of the equivalent S_q current system in the Northern Hemisphere is characterized by a dayside counterclockwise vortex [*Pedatella et al.*, 2011; *Yamazaki et al.*, 2011]. The current intensity was found to show a prominent annual variation with maximum in summer during solar minimum conditions and a semiannual variation with maxima at equinoxes during solar maximum [see *Campbell and Matsushita*, 1982; *Takeda*, 2002]. Thus, the S_q current system might cause negative auroral zone H component disturbances in the noon sector with seasonal dependence, as illustrated in

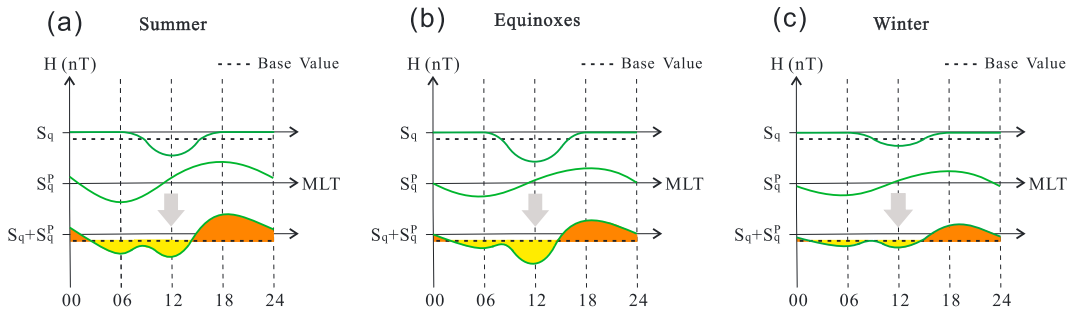

Figure 5. Sketch of expected MLT dependence of auroral zone H component disturbances caused by the Northern Hemisphere S_q and S_q^p current systems for (a) summer, (b) equinoxes, and (c) winter. The positive and negative perturbations caused by the combined effects are indicated by the orange and yellow shading, respectively.

the Figures 5a–5c (top). Note that the representative plots in Figure 5 show the average H disturbances over a complete solar cycle, without considering the solar cycle dependence. A base line for geomagnetic disturbances is generally determined by averaging all H values on the five internationally quiet days. Thus, the base values for the S_q effects should be negative, which are indicated by horizontal dashed lines.

The S_q^p current system is an equivalent current system inferred to explain the quiet day magnetic variations in the polar cap region. The morphology of the S_q^p current system in the Northern Hemisphere is characterized by a clockwise vortex in the dawnside and a counterclockwise in the duskside [*Tomita et al.*, 2011]. The current intensity was found to show an annual variation with maximum in summer [*Xu*, 1989]. Thus, the S_q^p current system might cause negative auroral zone H disturbances in the dawn sector and positive H disturbances in the dusk sector with seasonal dependence, as illustrated in Figures 5a–5c (middle). The base values for the S_q^p effects should be close to zero.

The combined effects of the S_q and S_q^p current systems are illustrated in Figures 5a–5c (bottom), in which the positive and negative H perturbations are indicated by the orange and yellow shading, respectively. Significant MLT and seasonal dependence can be seen in the combined effects. Moreover, as expected, they are consistent with the predominant features presented in Figure 4, except for the relatively weak annual variations in the *IU* index in the MLT sector 0400–0800. This suggests that most of these predominant features are mainly caused by the S_q and S_q^p current systems. The annual variations of the *IU* index in the MLT sector 0400–0800 might be associated with a dawn sector eastward current suggested by *Baumjohann and Kamide* [1981]. This eastward current is flowing equatorward of the auroral oval in a conductivity channel created by the precipitating electrons.

It is very clear that the quiet time current systems dominate over the electrojet currents in contributing to the geomagnetic perturbations recorded by the IMAGE magnetometers during quiet periods. Therefore, the IMAGE observations for quiet periods cannot be used to monitor the auroral electrojet activity. This is the reason we do not include quiet periods in the analysis of the MLT and seasonal variations in the electrojet currents in section 3.

Further, we examine the MLT and seasonal variations of the *IU* and *IL* indices and their latitudes (Lat-*IU* and Lat-*IL*) for disturbed periods having index values of more than 50 nT. The results are shown in Figure 6, where the standard deviations for the H component disturbances are less than 100 nT. Obviously, pronounced positive H perturbations in the MLT sector 1200–2200 and negative H perturbations in the MLT sector 2200–0600 are mainly associated with the auroral electrojets presented in Figure 2. The geomagnetic perturbations also appear in earlier local time sectors than those shown in Figure 2. For example, the positive H perturbations extend to the MLT sector ~0800–1200 during summer months and the negative H perturbations extend to the MLT sector ~1800–2200 during winter months. This implies that the electrojet currents are actually flowing in wider MLT sectors than those we concentrate on in this study. Although the magnetic signatures of the quiet time current systems do not appear, we believe that the quiet time current systems still contribute to the observed geomagnetic perturbations during disturbed periods, at least for the S_q currents, which are mainly controlled by the neutral tidal winds and the conductivities in the dynamo region [*Richmond et al.*, 1976]. The possible explanation might be that the contributions of the quiet time current systems are

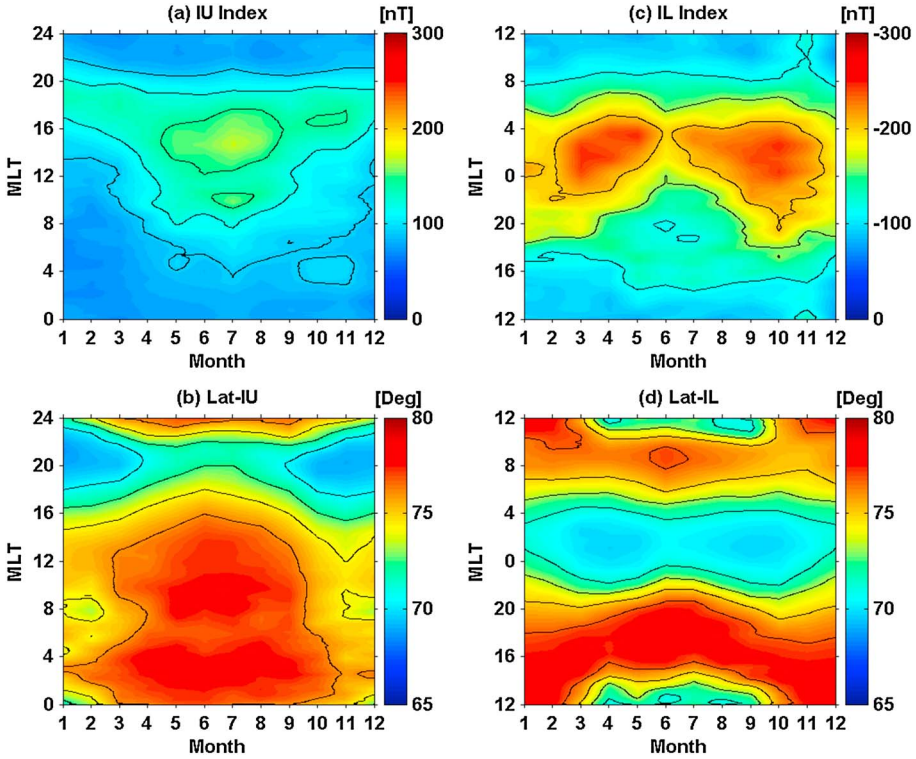

Figure 6. Same as Figure 4 but for disturbed periods having index values of more than 50 nT.

negligible when compared to those of the electrojet currents. If this is the case, the quiet time current systems would not significantly influence the results presented in Figure 2 for the disturbed periods.

5. Summary and Conclusions

The IMAGE network magnetic measurements offer the opportunity to delineate the MLT dependence of the auroral electrojets. In the present paper, the total eastward and westward electrojet currents (EEJ and WEJ) and their central latitudes (Lat-EEJ and Lat-WEJ) derived from the IMAGE network are analyzed to characterize the combined MLT and seasonal variations in the auroral electrojets for the period 1995–2009. Furthermore, the quiet time current effects, particularly the effects of the S_q and S_q^p current systems, are discussed in detail. It is found that the quiet time current systems dominate over the electrojet currents in contributing to the geomagnetic perturbations recorded by the IMAGE magnetometers during quiet periods.

We draw the following conclusions:

1. EEJ shows a strong MLT variation with significant dependence on season. During summer months the maxima occur around 1600–1800 MLT, whereas during winter months the maxima occur at a later local time sector around 1800–2000 MLT. Moreover, the summer maxima are much larger than the winter maxima and appear at higher latitudes. The summer maxima are mainly associated with the solar EUV conductivity effect, while the winter maxima are mainly due to the contribution of northward convective electric field.
2. EEJ exhibits a dominant annual variation with maximum in summer and minimum in winter. The amplitude of the annual variation significantly varies with MLT.
3. WEJ also exhibits a strong MLT variation with significant dependence on season. The maxima occur around 0200–0400 MLT during summer months, around 0000–0200 MLT during winter months, and in a wider local time sector around 0000–0400 MLT during equinoctial months. Moreover, the equinoctial maxima are much larger than the summer and winter maxima, and appear at relatively lower latitudes.
4. The seasonal variations in WEJ are the combinations of annual variations and semiannual variations. Both annual and semiannual variations show significant dependence on MLT.

Acknowledgments
This work is jointly supported by the Chinese Academy of Sciences (KZZD-EW-01-4), the 973 program (2012CB825601), the National Natural Science Foundation of China (41031066, 41231068,41204127, and 41374187), and the Specialized Research Fund for State Key Laboratories. J. Guo thanks the support by the NICT International Exchange Program and thanks Barbara A. Emery for her fruitful discussions. H.L. acknowledges support by JSPS grant-in-aid for scientific research (B) (25800274) and Shisedo Science grant. E.T. acknowledges the financial support by EU/FP7 ESPAS and the Academy of Finland to the ReSoLVE Centre of Excellence (272157). We thank the institutes who maintain the IMAGE Magnetometer Array.

Yuming Wang thanks Boris Kozelov and Octav Marghitu for their assistance in evaluating this paper.

References

Ahn, B.-H., B. Emery, H. Kroehl, and Y. Kamide (1999), Climatological characteristics of the auroral ionosphere in terms of electric field and ionospheric conductance, *J. Geophys. Res.*, *104*(A5), 10,031–10,040.

Ahn, B.-H., H. Kroehl, Y. Kamide, and E. Kihn (2000), Seasonal and solar cycle variations of the auroral electrojet indices, *J. Atmos. Sol. Terr. Phys.*, *62*, 1301–1310.

Allen, J. H., and H. W. Kroehl (1975), Spatial and temporal distributions of magnetic effects of auroral electrojets as derived from *AE* indices, *J. Geophys. Res.*, *80*, 3667–3677.

Amm, O., and A. Viljanen (1999), Ionospheric disturbance magnetic field continuation from the ground to the ionosphere using spherical elementary current systems, *Earth Planets Space*, *51*, 431–440.

Baumjohann, W., and Y. Kamide (1981), Joint two-dimensional observations of ground magnetic and ionospheric electric fields associated with auroral zone currents 2. Three-dimensional current flow in the morning sector during substorm recovery, *J. Geomag. Geoelectr.*, *33*, 297–318.

Cliver, E. W., Y. Kamide, and A. G. Ling (2000), Mountains versus valleys: Semiannual variation of geomagnetic activity, *J. Geophys. Res.*, *105*, 2413–2424.

Campbell, W. H., and S. Matsushita (1982), S_q currents: A comparison of quiet and active year behavior, *J. Geophys. Res.*, *87*(A7), 5305–5308.

Davis, T. N., and M. Sugiura (1966), Auroral electrojet activity index *AE* and its universal time variations, *J. Geophys. Res.*, *71*(3), 785–801, doi:10.1029/JZ071i003p00785.

Finch, I. D., M. L. Lockwood, and A. P. Rouillard (2008), Effects of solar wind magnetosphere coupling recorded at different geomagnetic latitudes: Separation of directly-driven and storage/release systems, *Geophys. Res. Lett.*, *35*, L21105, doi:10.1029/2008GL035399.

Gjerloev, J. W. (2009), A global ground-based magnetometer initiative, *Eos Trans. AGU*, *90*(27), 230–231, doi:10.1029/2009EO270002.

Gjerloev, J. W., R. A. Hoffman, M. M. Friel, L. A. Frank, and J. B. Sigwarth (2004), Substorm behavior of the auroral electrojet indices, *Ann. Geophys.*, *22*, 2135–2149, doi:10.5194/angeo-22-2135-2004.

Guo, J., X. Feng, T. I. Pulkkinen, E. I. Tanskanen, W. Xu, J. Lei, and B. A. Emery (2012), Auroral electrojets variations caused by recurrent high-speed solar wind streams during the extreme solar minimum of 2008, *J. Geophys. Res.*, *117*, A04307, doi:10.1029/2011JA017458.

Guo, J., T. I. Pulkkinen, E. I. Tanskanen, X. Feng, B. A. Emery, H. Liu, C. Liu, and D. Zhong (2014), Annual variations in westward auroral electrojet and substorm occurrence rate during solar cycle 23, *J. Geophys. Res. Space Physics*, *119*, doi:10.1002/2013JA019742.

Juusola, L., K. Kauristie, O. Amm, and P. Ritter (2009), Statistical dependence of auroral ionospheric currents on solar wind and geomagnetic parameters from 5 years of CHAMP satellite data, *Ann. Geophys.*, *27*, 1005–1017.

Kallio, E. I., T. I. Pulkkinen, H. E. J. Koskinen, A. Viljanen, J. A. Slavin, and K. Ogilvie (2000), Loading-unloading processes in the nightside ionosphere, *Geophys. Res. Lett.*, *27*(11), 1627–1630, doi:10.1029/1999GL003694.

Kamide, Y., and S.-I. Akasofu (1983), Notes on the auroral electrojet indices, *Rev. Geophys. Space Phys.*, *21*, 1647–1656.

Kauristie, K., T. I. Pulkkinen, R. J. Pellinen, and H. J. Opgenoorth (1996), What can we tell about global auroral-electrojet activity from a single meridional magnetometer chain?, *Ann. Geophys.*, *14*, 1177–1185.

Liou, K., K. Takahashi, B. J. Anderson, M. Nose, and T. Iyemori (2013), Assessment of the auroral electrojet index performance under various geomagnetic conditions, *J. Atmos. Sol. Terr. Phys.*, *92*, 31–36.

Lyatsky, W., P. T. Newell, and A. Hamza (2001), Solar illumination as cause of the equinoctial preference for geomagnetic activity, *Geophys. Res. Lett.*, *28*, 2353–2356, doi:10.1029/2000GL012803.

Moretto, T., N. Olsen, P. Ritter, and G. Lu (2002), Investigating the auroral electrojets with low altitude polar orbiting satellites, *Ann. Geophys.*, *20*, 1049–1061.

Newell, P. T., T. Sotirelis, J. P. Skura, C.-I. Meng, and W. Lyatsky (2002), Ultraviolet insolation drives seasonal and diurnal space weather variations, *J. Geophys. Res.*, *107*(A10), 1305, doi:10.1029/2001JA000296.

Newell, P. T., and J. W. Gjerloev (2011), Evaluation of SuperMAG auroral electrojet indices as indicators of substorms and auroral power, *J. Geophys. Res.*, *116*, A12211, doi:10.1029/2011JA016779.

Pedatella, N. M., J. M. Forbes, and A. D. Richmond (2011), Seasonal and longitudinal variations of the solar quiet (S_q) current system during solar minimum determined by CHAMP satellite magnetic field observations, *J. Geophys. Res.*, *116*, A04317, doi:10.1029/2010JA016289.

Pulkkinen, A., O. Amm, and A. Viljanen (2003), Ionospheric equivalent current distributions determined with the method of spherical elementary current systems, *J. Geophys. Res.*, *108*(A2), 1053, doi:10.1029/2001JA005085.

Pulkkinen, T. I., E. I. Tanskanen, A. Viljanen, N. Partamies, and K. Kauristie (2011), Auroral electrojets during deep solar minimum at the end of solar cycle 23, *J. Geophys. Res.*, *116*, A04207, doi:10.1029/2010JA016098.

Richmond, A. D., S. Matsushita, and J. D. Tarpley (1976), On the production mechanism of electric currents and fields in the ionosphere, *J. Geophys. Res.*, *81*(4), 547–555.

Russell, C. T., and R. L. McPherron (1973), Semiannual variation of geomagnetic activity, *J. Geophys. Res.*, *78*, 92–108.

Singh, A. K., R. Rawat, and B. M. Pathan (2013), On the UT and seasonal variations of the standard and SuperMAG auroral electrojet indices, *J. Geophys. Res. Space Physics*, *118*, 5059–5067, doi:10.1002/jgra.50488.

Svalgaard, L. (1977), Geomagnetic activity: Dependence on solar wind parameters, in *Coronal Holes and High Speed Wind Streams*, edited by J. B. Zirker, 371 pp., Colorado Associated Univ. Press, Boulder, Colo.

Takeda, M. (2002), Features of the global geomagnetic S_q field from 1980 to 1990, *J. Geophys. Res.*, *107*(A9), 1252, doi:10.1029/2001JA009210.

Tanskanen, E. I. (2009), A comprehensive high-throughput analysis of substorms observed by IMAGE magnetometer network: Years 1993–2003 examined, *J. Geophys. Res.*, *114*, A05204, doi:10.1029/2008JA013682.

Tanskanen, E. I., T. I. Pulkkinen, A. Viljanen, K. Mursula, N. Partamies, and J. A. Slavin (2011), From space weather toward space climate time scales: Substorm analysis from 1993 to 2008, *J. Geophys. Res.*, *116*, A00I34, doi:10.1029/2010JA015788.

Tomita, S., et al. (2011), Magnetic local time dependence of geomagnetic disturbances contributing to the AU and AL indices, *Ann. Geophys.*, *29*, 673–678.

Vennerstrom, S., and T. Moretto (2013), Monitoring auroral electrojets with satellite data, *Space Weather*, *11*, 509–519, doi:10.1002/swe.20090.

Viljanen, A., and L. Häkkinen (1997), IMAGE magnetometer network, in *Satellite-ground Based Coordination Sourcebook*, edited by M. Lockwood, M. N. Wild, and H. J. Opgenoorth, pp. 111–117, Eur. Space Agency Spec. Publ., ESA-SP, 1198, Fennoscandia and Svalbard.

Xu, W.-Y. (1989), Polar region S_q, *Pure Appl. Geophys.*, *113*, 371–393.
Yamazaki, Y., et al. (2011), An empirical model of the quiet daily geomagnetic field variation, *J. Geophys. Res.*, *116*, A10312, doi:10.1029/2011JA016487.
Zhao, H., and Q.-G. Zong (2012), Seasonal and diurnal variation of geomagnetic activity: Russell-McPherron effect during different IMF polarity and/or extreme solar wind conditions, *J. Geophys. Res.*, *117*, A11222, doi:10.1029/2012JA017845.